scientific reports

Check for updates

OPEN

Spatial interaction between retinal and choroidal circulation in retinal vein occlusion

SolAh Han[1], Sang Uk Choi[1], Yoon Jeon Kim[1], Young Hee Yoon[1] & Junyeop Lee[1,2]✉

Retinal vein occlusion (RVO) is a leading cause of vision loss, yet the interaction between retinal and choroidal circulation in this condition remains incompletely understood. This retrospective, cross-sectional study aimed to quantitatively evaluate choroidal structural changes in treatment-naïve unilateral RVO using ultra-widefield imaging. Twenty-nine patients with unilateral branch or central RVO and their unaffected fellow eyes were analyzed. Mean choroidal thickness (MCT) and choroidal vascular index (CVI) were measured on widefield swept-source optical coherence tomography, while choroidal vascular density (CVD) and choroidal vascular fractal dimension (CFD) were calculated from ultra-widefield indocyanine green angiography (UWF-ICGA) images using binarization and fractal analysis protocols. Compared with fellow eyes, RVO eyes demonstrated significantly increased MCT (254.48 ± 60.72 µm vs. 230.68 ± 60.47 µm, $P = 0.030$), CVI (64.85 ± 3.38 vs. 61.88 ± 4.34, $P = 0.011$), and CVD (62.24 ± 2.87 vs. 60.01 ± 3.41, $P = 0.038$), whereas CFD was reduced (1.77 ± 0.02 vs. 1.82 ± 0.02, $P < 0.001$). Sub-quadrant analysis in branch RVO revealed that choroidal vascular changes were localized to the affected quadrant, with significantly higher CVD and lower CFD than the corresponding quadrants in the same and fellow eyes. These findings suggest that RVO induces regional choroidal vascular remodeling, possibly mediated by VEGF-driven vasodilation and inflammatory pathways, supporting a spatially localized interaction between retinal and choroidal circulation in acute retinal vascular occlusion.

Keywords Retinal vein occlusion, Choroidal vascular remodeling, Choroidal vascular density, Choroidal vascular fractal dimension, Ultra-widefield imaging

Within the spectrum of retinal vascular disorders, retinal vein occlusion (RVO) represents a major cause of visual impairment worldwide[1,2]. RVO is characterized by obstruction of retinal venous circulation, leading to retinal ischemia, macular edema, and progressive visual loss[2]. The clinical presentation, prognosis, and therapeutic response are influenced by both the site of venous occlusion and the extent of retinal nonperfusion. Previous investigations employing enhanced depth imaging optical coherence tomography (ECI-OCT) have demonstrated that patients with RVO exhibit increased choroidal thickness[3]. Furthermore, other studies have suggested that alterations in choroidal structure may serve a predictive markers for disease severity and visual prognosis of RVO[4–6].

The choroid, a vascular layer situated beneath the retina, plays a critical role in supplying oxygen and nutrients to the outer retina. Alterations in choroidal circulation are well recognized pathogenesis of several retinal disorders. Choroidal neovascularization is a hallmark of exudative age-related macular degeneration (AMD),[7] and central serous chorioretinopathy (CSC) has been closely linked to choroidal abnormalities, as demonstrated by hyperpermeability in indocyanine green angiography (ICGA) and increased choroidal thickness on OCT[8,9]. in addition, dysregulation of choroidal blood flow has been implicated in diabetic retinopathy[10,11]. Collectively, these conditions highlight the essential role of the choroidal vasculature in retinal disease. While exudative AMD, CSC and diabetic retinopathy are diseases that directly involve or significantly impact choroidal circulation, the role of the choroid in primarily retinal vascular disorders such as RVO remain less clearly defined. The investigation of choroidal changes in RVO may therefore provide important insight into its pathophysiology, clinical course, and prognosis.

[1]Department of Ophthalmology, Asan Medical Center, College of Medicine, University of Ulsan, 88 Olympic-ro 43-gil, Songpa-gu, Seoul 05505, South Korea. [2]Graduate School of Health Science and Technology, Ulsan National Institute of Science & Technology (UNIST), 50 UNIST-gil, Eonyang-eup, Ulju-gun, Ulsan 44919, South Korea. ✉email: j.lee@amc.seoul.kr

	RVO
N.	29
BRVO	22 (75.9%)
CRVO	7 (24.1%)
Age (yr)	61.2 ± 12.0
Sex	
Female	19 (65.5%)
Male	10 (34.4%)
LogMAR VA	0.41 ± 0.40
IOP (mmHg)	15.6 ± 3.2
Systemic disease	
HTN	15 (51.7%)
DM	6 (20.7%)
Dyslipidemia	5 (17.2%)
Coronary heart disease	3 (10.3%)

Table 1. Baseline characteristics and clinical characteristics of patients with retinal vein occlusion patients (RVO).

		RVO eye ($n=29$)	Fellow eye ($n=29$)	*P* value
UWF OCT	Mean Choroidal Thickness (MCT, um)	254.48 ± 60.72	230.68 ± 60.47	0.030*
	Choroidal Vascular Index (CVI, %)	64.85 ± 3.38	61.88 ± 4.34	0.011*
UWF ICGA	Choroidal Vascular Density (CVD, %)	62.24 ± 2.87	60.01 ± 3.41	0.038*
	Choroidal Vascular Fractal Dimension (CFD)	1.77 ± 0.02	1.82 ± 0.02	< 0.001*

Table 2. Comparison of ultrawide field optical coherence tomography (UWF OCT) and indocyanine green angiography (UWF ICGA) parameters between eyes with retinal vein occlusion (RVO) and fellow eyes. Mann-Whitney test (*statistically significant).

RVO is a well-recognized retinal vascular disorder characterized by venous obstruction, resulting in retinal edema, hemorrhage, and inflammation[12]. Although the retinal manifestations of RVO have been extensively investigated, critical gap remains in our understanding of how retinal fluid dynamics influence the choroid, as well as the role of inflammation in mediating choroidal vascular alterations[13–15]. By analyzing ultra-widefield indocyanine green angiography (UWF-ICGA) images from patients with RVO, the present study seeks to elucidate the interaction between retinal and choroidal circulations, thereby contributing to a more comprehensive understanding of RVO pathophysiology.

Results

The baseline characteristics of the study population are summarized in Table 1. A total of 29 patients with RVO were included in this study. Among the affected eyes, 22 (75.9%) had BRVO and 7 (24.1%) had central retinal vein occlusion (CRVO). The 29 unaffected fellow eyes served as controls. The mean age of the patients was 61.2 ± 12.0years, and 34.4% were male. Hypertension was most common systemic comorbidity (Table 1 and 51.7%) followed by DM (20.7%) and dyslipidemia (17.2%).

Choroidal structural and vascular parameters in RVO versus fellow eyes

The MCT was significantly greater in RVO eyes compared with fellow eyes (254.48 ± 60.72 μm vs. 230.68 ± 60.47 μm, $P=0.030$; Table 2). Similarly, the CVI was higher in RVO eyes than in fellow eyes (64.85 ± 3.38 vs. 61.88 ± 4.34, $P=0.011$; Table 2). In UWF ICGA image analysis, RVO eyes demonstrated significantly higher CVD than fellow eyes (62.24 ± 2.87 vs. 60.01 ± 3.41, $P=0.038$; Fig. 4A, C; Table 2,). In contrast, CFD, which reflects vascular complexity, was significantly lower in RVO eyes compared with fellow eyes (1.77 ± 0.02 vs. 1.82 ± 0.02, $P<0.001$; Fig. 4E, G; Table 2).

Sub-quadrant analysis of BRVO eyes

In sub-quadrant analysis of BRVO patients, the affected quadrant exhibited significantly higher CVD and lower CFD compared with both horizontally symmetric quadrant in the fellow eye (Fig. 4B, D, F, H; Table 3 Comparison A) and the vertically symmetric quadrant within the same RVO eye (Table 3 Comparison B). By contrast, the unaffected, vertically symmetric quadrant in the RVO eye did not differ significantly in CVD or CFD compared with the corresponding horizontally symmetric quadrant in the fellow eye (Table 3 comparison C). Similarly, in fellow eyes, comparisons between horizontally and vertically symmetric quadrants showed no significant differences in CVD and CFD (Table 3 comparison D). Taken together, these findings indicate that RVO eyes are

		BRVO eye ($n=22$)	Fellow eye ($n=22$)	*P* value
Comparison A (affected Q vs. horizontally symmetric)	CVD (%)	62.56 ± 0.53	61.57 ± 1.38	0.003*
	CFD	1.795 ± 0.018	1.807 ± 0.015	0.015*
Comparison B (affected Q vs. vertically symmetric)	CVD (%)	62.56 ± 0.53	61.75 ± 1.38	0.021*
	CFD	1.795 ± 0.018	1.818 ± 0.020	0.010*
Comparison C (vertically symmetric Q vs. its horizontally symmetric)	CVD (%)	61.75 ± 1.38	61.84 ± 1.63	0.741
	CFD	1.818 ± 0.020	1.809 ± 0.015	0.098
Comparison D (horizontally symmetric Q vs. its vertically symmetric)	CVD (%)	61.57 ± 1.38	61.84 ± 1.63	0.728
	CFD	1.807 ± 0.015	1.809 ± 0.015	0.749

Table 3. Sub-quadrant comparison of choroidal vascular density (CVD) and choroidal vascular fractal dimension (CFD) between eyes with branch retinal vascular occlusion (BRVO) eye and fellow eyes. Mann-Whitney test (*statistically significant). Comparison A: Affected quadrant (Q) in the BRVO eye vs. the horizontally symmetric Q in fellow eye (Fig. 3, quadrant A vs. quadrant B); Comparison B: Affected Q in the BRVO eye vs. the vertically symmetric Q in the same eye (Fig. 3, quadrant A vs. quadrant C); Comparison C: Vertically symmetric Q in the BRVO eye vs. the corresponding horizontally symmetric Q in the fellow eye (Fig. 3, quadrant C vs. quadrant D); Comparison D: Horizontally symmetric Q in the fellow eye vs. its vertically symmetric Q in the same eye (Fig. 3, quadrant B vs. quadrant D).

characterized by increased choroidal thickness and vascular density, but reduced vascular complexity, with these changes being most pronounced in the affected quadrants of BRVO eyes.

Discussion

In this study, we demonstrated that eyes with RVO exhibit significant alterations in choroidal structure and vascularity compared with fellow eyes. Specifically, RVO eyes showed increased mean choroidal thickness and choroidal vascular index, as well as elevated choroidal vascular density. Conversely, choroidal vascular fractal dimension, a measure of vascular branching complexity, was reduced in RVO eyes, suggesting a shift toward a less complex vascular architecture. These changes were most pronounced within the affected quadrants of BRVO eyes, whereas unaffected quadrants showed no significant differences.

Recent studies have suggested that structural and functional alterations of the choroid may occur during the clinical course of RVO; however, extrafoveal choroidal vascular changes have not been well characterized[16–18]. In the present study, we demonstrated, through quantitative image analysis, that RVO is associated with spatial interactions between the retina and choroidal circulation. Specifically, RVO eyes exhibited increased CVD and decreased CFD compared with fellow eyes. Unlike diabetic retinopathy, in which chronic retinal ischemia directly influences both retinal and choroidal circulations, RVO is primarily an acute venous occlusive event that compromises inner retinal perfusion[19–21]. Nevertheless, our findings suggest a localized complementary relationship between retinal and choroidal circulation in the setting of RVO.

RVO is a localized retinal pathology caused by venous occlusion, leading to retinal hemorrhage, edema, and, in cases involving the macula, vision-threatening macular edema[1,12]. The mainstay treatments for macular edema associated with RVO include intravitreal anti-VEGF (vascular endothelial growth factor) injection and corticosteroid injections, reflecting the central role of VEGF expression and inflammation in visual loss following venous occlusion[2,14]. Although VEGF and inflammatory cytokines were traditionally thought to exert only regional effects, accumulating evidence suggests that they may diffuse throughout the vitreous cavity, influencing the entire retina and choroid[4,15,17]. Previous studies have shown that levels of angiogenic and inflammatory cytokines correlate strongly with the degree of retinal ischemia in RVO[22]. Consistent with this, our earlier work demonstrated that retinal ischemia induces choroidal vascular dilation and hyperpermeability via the vascular endothelial growth factor-A-plasmalemma vesicle-associated protein axis[23]. The spatial correspondence between retinal and choroidal alterations observed in the present study suggest that changes in intraocular angiogenic and inflammatory mediators may contribute to coordinated vascular responses across both circulations.

Our results are consistent with previous studies. Mitamura et al. reported increased sub-foveal choroidal thickness in treatment naïve RVO eyes[4], and using OCT, demonstrated that both total choroidal area and stromal area were greater than those of fellow eyes. These changes were attributed to VEGF-driven vascular leakage[4,24]. Similarly, our study revealed that MCT and CVI were increased in RVO eyes relative to fellow eyes, supporting the presence of choroidal structural remodeling. Importantly, by extending the analysis beyond the subfoveal region, we were able to demonstrate that RVO induces structural alterations within the choroidal vasculature, including increased CVD and decreased CFD, with the most pronounced alterations localized to the RVO-affected quadrant.

Although the choroidal parameters differed significantly between RVO and fellow eyes, the absolute magnitudes of these differences were modest, suggesting that these changes likely represent subtle microvascular alterations rather than large or clinically immediate effects. Despite the small effect sizes, the consistent directional pattern—thicker choroid, higher vascular density, and reduced fractal complexity across whole-eye and quadrant-level analyses—supports a biologically plausible trend toward localized choroidal remodeling in areas affected by venous obstruction.

The more substantial reduction in CFD compared with the modest increase in CVD further clarifies the nature of these alterations. While dilation of medium- to large-caliber vessels may slightly increase total luminal area, the loss or simplification of small vessel branching produces a disproportionately greater decline in vascular complexity. One interpretation is that structural simplification—including loss of small-caliber branches—may occur earlier or more prominently than choroidal vasodilation in the context of RVO, indicating a localized structural response of the choroid to acute retinal circulatory compromise. Given the retrospective and cross-sectional design, however, the clinical implications of these findings cannot be fully determined. Longitudinal studies with larger cohorts will be essential to evaluate whether choroidal vascular alterations influence disease progression, visual outcomes, or treatment response.

Moreover, studies have shown that patients with RVO and serous retinal detachment exhibit greater choroidal thickness than those without retinal detachment[16], suggesting that regional alterations in retinal vasculature can extend to the choroid. In our sub-quadrant analysis, only the affected quadrant demonstrated significantly increased CVD and decreased CFD compared with the corresponding fellow eye quadrant, while non-affected quadrants showed no differences. This spatial correspondence provides strong evidence that RVO induces localized choroidal vascular remodeling in regions directly impacted by retinal circulation compromise.

Although the present study did not assess the relationship between choroidal parameters and visual acuity or treatment response, previous work has shown that anti-VEGF or corticosteroid treatment for RVO-related macular edema may not uniformly affect choroidal thickness or vascular metrics[18]. Other studies have noted subtype-specific differences, with CRVO and BRVO demonstrating distinct patterns of choroidal response following therapy[25]. These observations suggest that underlying differences in pathogenesis between BRVO and CRVO may influence choroidal vascular changes after treatment.

The choroid is known to be influenced by multiple factors, including age, axial length, refractive error, and diurnal variation[26]. By comparing RVO eyes with fellow eyes, we minimized the influence of such confounders. Nonetheless, our study has several limitations. First, the relatively small sample size, particularly the small subgroup of CRVO eyes, limits the statistical power of our conclusions. A larger, prospective study is warranted to confirm these findings and to perform a robust sub-analysis of different RVO types. Second, VEGF and inflammatory cytokine levels in aqueous or vitreous samples were not measured, precluding direct correlation between intraocular mediator levels and choroidal vascular changes. Third, UWF ICGA images were analyzed without stereographic projection software, which may have led to overestimation of peripheral vascular parameters. Finally, due to the cross-sectional design, we were unable to determine whether the observed choroidal vascular alterations are reversible.; longitudinal studies, particularly those including post-treatment imaging, are needed to clarify this issue.

In conclusion, this study identifies regionally confined alterations in choroidal vascular structure that are associated with the areas of retinal involvement in RVO. The localized increase in CVD and decrease in CFD in affected quadrants suggest that choroidal vascular remodeling may serve a compensatory role in the context of impaired retinal circulation. These findings provide novel evidence for spatial interactions between retinal and choroidal vasculature and highlight the importance of considering choroidal circulation in the pathophysiology of acute retinal vascular disease.

Methods

Study participants

This retrospective cross-sectional observational study was conducted in the Department of Ophthalmology of Asan Medical Center in Seoul, South Korea, in accordance with the tenets of the Declaration of Helsinki. The study was approved by the Institutional Review Board (IRB) of Asan Medical Center, Seoul, South Korea and informed consent was obtained from all subjects involved in the study. Treatment-naïve patients with unilateral RVO who presented to our clinic and underwent UWF ICGA within 3 months of symptom onset were included. The fellow eyes of these patients were used as controls. The exclusion criteria were as follows: (1) eyes with a history of any intraocular surgery other than uncomplicated cataract surgery, ocular trauma, intravitreal injection, and ocular laser treatment; (2) presence of other retinal or choroidal diseases, including glaucoma, age-related macular degeneration, diabetic retinopathy, hypertensive retinopathy, or pachychoroid spectrum disease[27]; (3) a history of uveitis and bilateral RVO; (4) significant media opacity interfering with image analysis; (5) refractive errors larger than ± six diopters (as a spherical equivalent). The same exclusion criteria were applied to the fellow eyes.

All subjects underwent a comprehensive general medical evaluation and a detailed ophthalmologic examination, including a best-corrected visual acuity (BCVA), non-contact pneumatic tonometry, dilated fundus examination, slit-lamp microscopy, widefield swept-source OCT (Optos Silverstone: Optos PLC; Dunfermline, UK), UWF fluorescein angiography, and UWF ICGA (Optos California: Optos PLC, Dunfermline, UK).

Image analysis

Measurement of mean choroidal thickness (MCT) and choroidal vascular index (CVI)

Widefield swept-source OCT (Optos Silverstone: Optos PLC; Dunfermline, UK) with a 1050-nm wavelength light source and a A-scan rate up to 100,000 cycles/second was used for image acquisition. The maximum line scan length was 23 mm. For each eye, a 23 horizontal line scan passing through the fovea was obtained. The mean choroidal thickness (MCT) was calculated as the average of choroidal thickness measured at four points: the foveal center, 3000 μm nasal to the fovea, 3000 μm temporal to the fovea, and 6000 μm temporal to the fovea (Fig. 1, upper row). Choroidal thickness and CVI were measured at 3000 μm nasal and 6000 μm temporal to the fovea to capture the widest obtainable horizontal extent of the choroid. Choroidal thickness was defined as the vertical distance from the outer margin of the hyperreflective retinal pigment epithelium (RPE) line to the choroid-scleral junction[28,29] (Fig. 1, upper row). Measurements were performed independently by two retinal

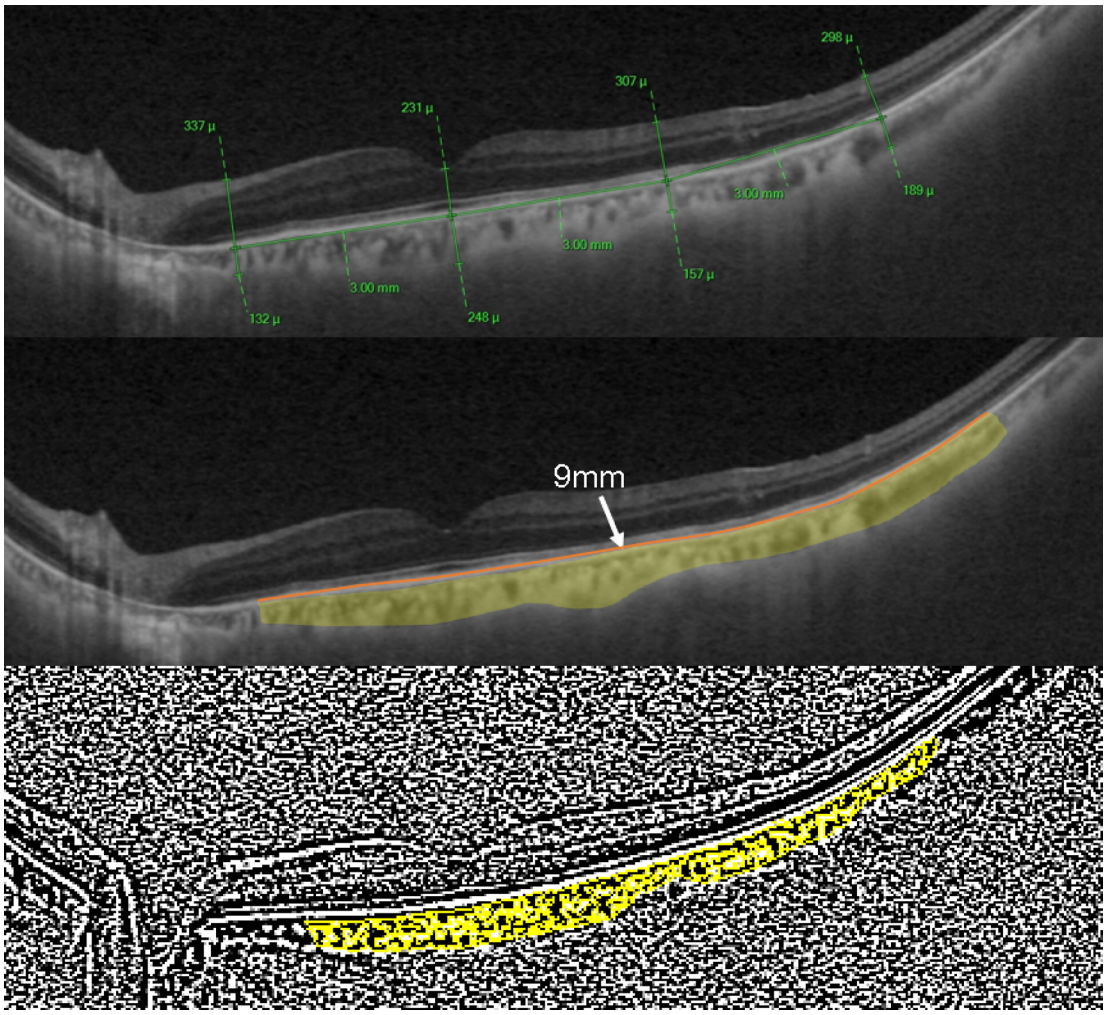

Fig. 1. Measurement of mean choroidal thickness (MCT) and choroidal vascular index (CVI). MCT was determined using the built-in caliper tool on swept-source OCT (upper row) and CVI was calculated using Image J software through binarization and segmentation process (middle and lower rows).

specialists (S.U.C and J.L) using the built-in caliper tool (Optos Advance, Optos PLC; Dunfermline, UK). The CVI was calculated according previously described protocols[30]. For CVI analysis, the region from 3000 µm nasal to 6000 µm temporal to the fovea along the 23-mm horizontal line scan was used. Image binarization was performed using ImageJ version 1.53 h (National Institute of Health, Bethesda, MD, USA; https://imagej.nih.gov/ij/). The choroidal area was delineated using the polygon selection tool, and the regions of interest (ROI) were added to the ROI manager. Images were converted to a 8-bit and processed with Niblack's auto local thresholding tool. The stromal area was highlighted and added to the ROI manager (Fig. 1, third row). The polygonal choroidal area and stromal area were combined using the "AND" operation in the ROI manager to generate a third ROI. The luminal area was determined by subtracting the stromal area from the total choroidal area. CVI was calculated as the ratio of luminal area to choroidal area.

Analysis of choroidal vascular density (CVD) and choroidal vascular fractal dimension (CFD)

UWF FA and ICGA were performed after informed consent was obtained. For analysis, early-phase UWF-ICGA images (between 1 and 2 min after the injection of dye) were used. CVD and CFD was quantified using ImageJ software version 1.53 h (https://imagej.nih.gov/ij/, National Institute of Health, Bethesda, MD, USA) with modified protocols from previous studies (Fig. 2)[11,29,31]. Two retinal specialists (S.U.C and J.L.) delineated an oval ROI (3200 × 2400 pixels) centered on the fovea. Niblack's auto local thresholding was applied to binarize images, and the color threshold tool was used to isolate the luminal area (Fig. 2C). CFD was calculated using the FracLac plug-in for Image J (https://imagej.nih.gov/ij/plugins/fraclac/fraclac.html; Fig. 2D).

Quadrant sub-analysis in BRVO patients

For eyes with branch retinal vein occlusion (BRVO), the oval ROI was divided into 4 quadrants for sub-analysis of CVI and CFD (Fig. 3). The quadrant corresponding to the site of RVO was designated as the "affected quadrant".

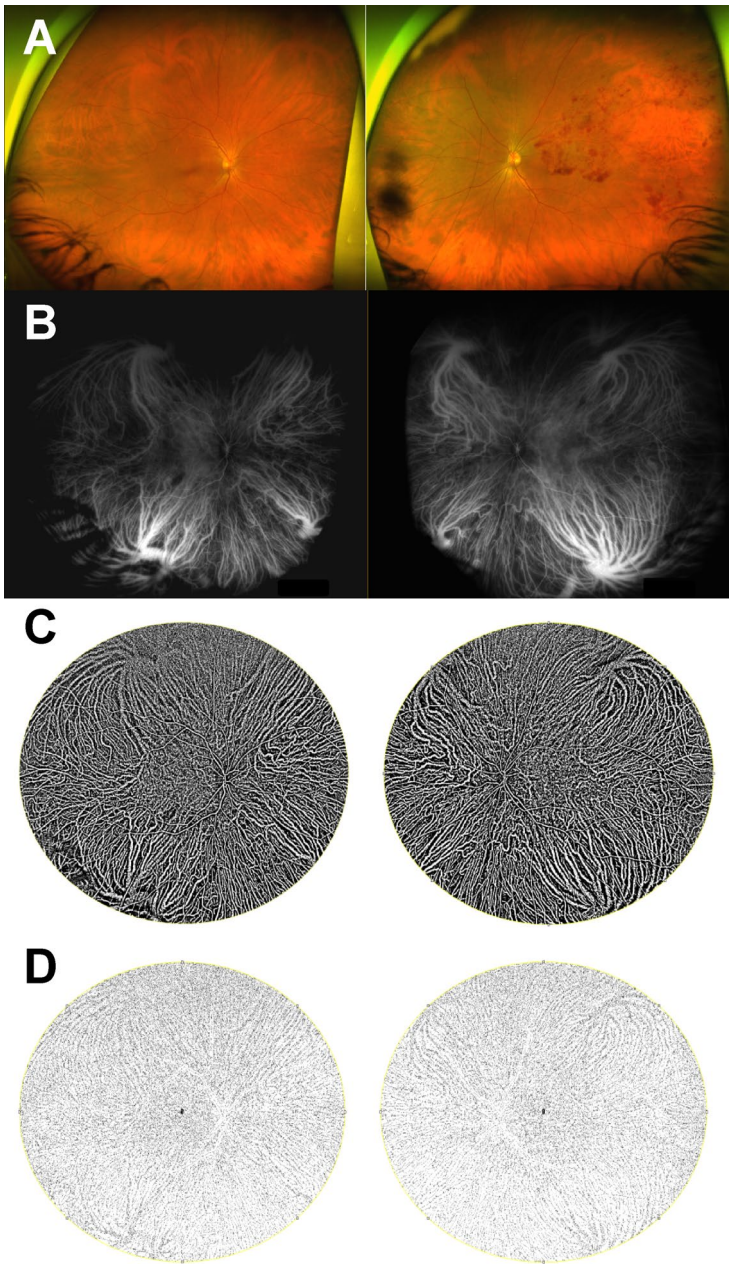

Fig. 2. Image processing workflow for analysis of choroidal vascular density (CVD) and choroidal vascular fractal dimension (CFD) in a retinal vein occlusion (RVO) eye and its fellow eye. (**A**) Widefield fundus photograph, (**B**) ultra-widefield indocyanine green angiography (ICGA) image, (**C**) binarized image and threshold adjustment for CVD measurement, (**D**) fractal analysis using the FracLac plug-in for CFD measurement.

Multiple comparisons were performed as follows (Table 3): (Comparison A) affected quadrant of the RVO eye vs. the corresponding quadrant of the fellow eye (e.g. superotemporal quadrant in RVO eye vs. superotemporal quadrant in the fellow eye); (Comparison B) affected quadrant of the RVO eye vs. its vertically symmetric quadrant in the same eye (e.g. superotemporal vs. inferotemporal quadrant in RVO eye); (Comparison C) vertically symmetric quadrant of the affected quadrant in the RVO eye vs. the corresponding quadrant in the fellow eye (e.g. inferotemporal quadrant in RVO eye vs. inferotemporal quadrant in fellow eye); (Comparison D) horizontally symmetric quadrant vs. vertically symmetric quadrant in the fellow eye (e.g. superotemporal vs. inferotemporal quadrant in the fellow eye). To ensure consistency, all ICGA images were processed using an identical ImageJ macro that applied uniform binarization and skeletonization steps to both RVO and fellow eyes. Because the same quadrant-based segmentation was applied symmetrically to each pair, anatomical variations would equally affect both eyes within a subject, minimizing their impact on intra-individual comparisons (Fig. 4).

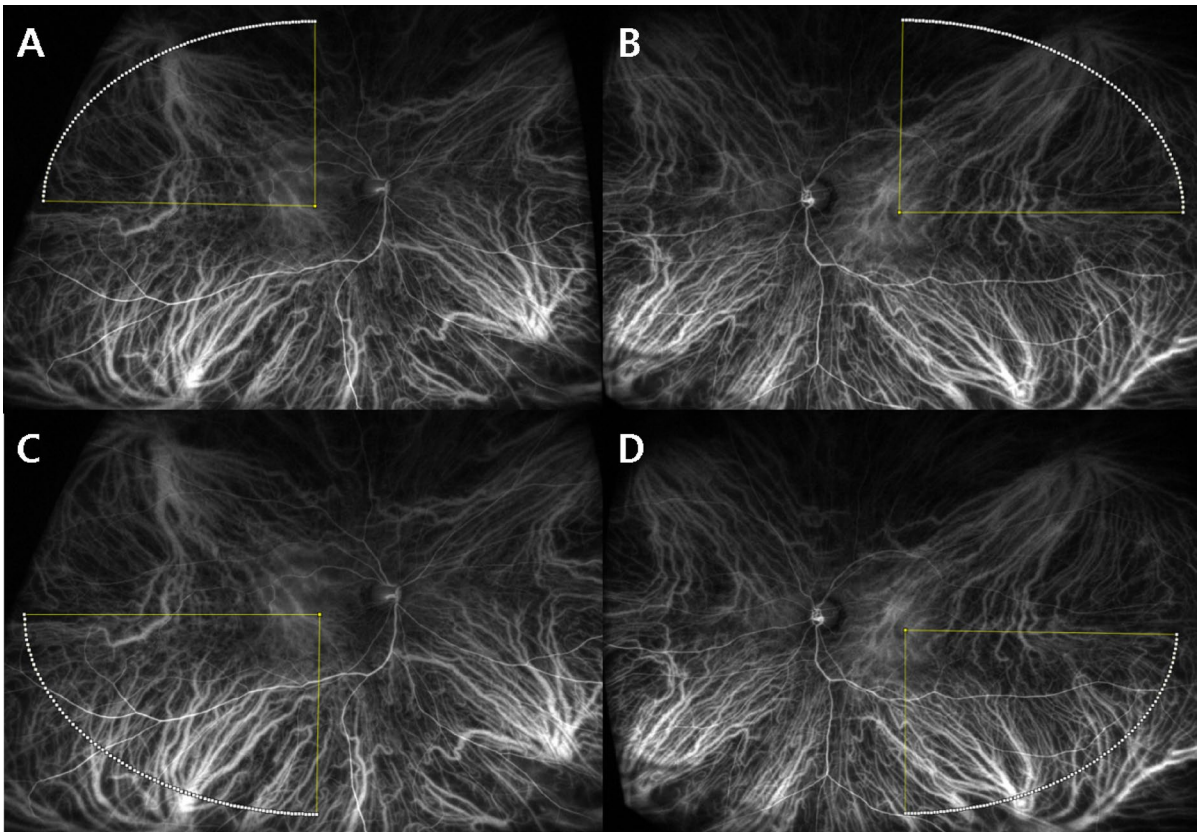

Fig. 3. Quadrant sub-analysis of ultra-widefield indocyanine green angiography (ICGA) images. Each image was divided into four quadrants to compare choroidal vascular parameters between the affected quadrant in retinal vein occlusion (RVO) eyes and corresponding quadrants in fellow eyes.

Statistical analysis

All statistical analyses were performed using the Statistical Package for the Social Sciences (SPSS), version 21.0 (IBM Co., Armonk, New York, USA). Continuous variables were presented as mean ± standard deviation (SD), and categorical variables were summarized as counts (n) and percentages (%). comparisons of continuous variables were conducted using the Mann-Whitney U test and categorical variables were compared using Fisher's exact test. A two-sided p-value of less than 0.05 was considered statistically significant.

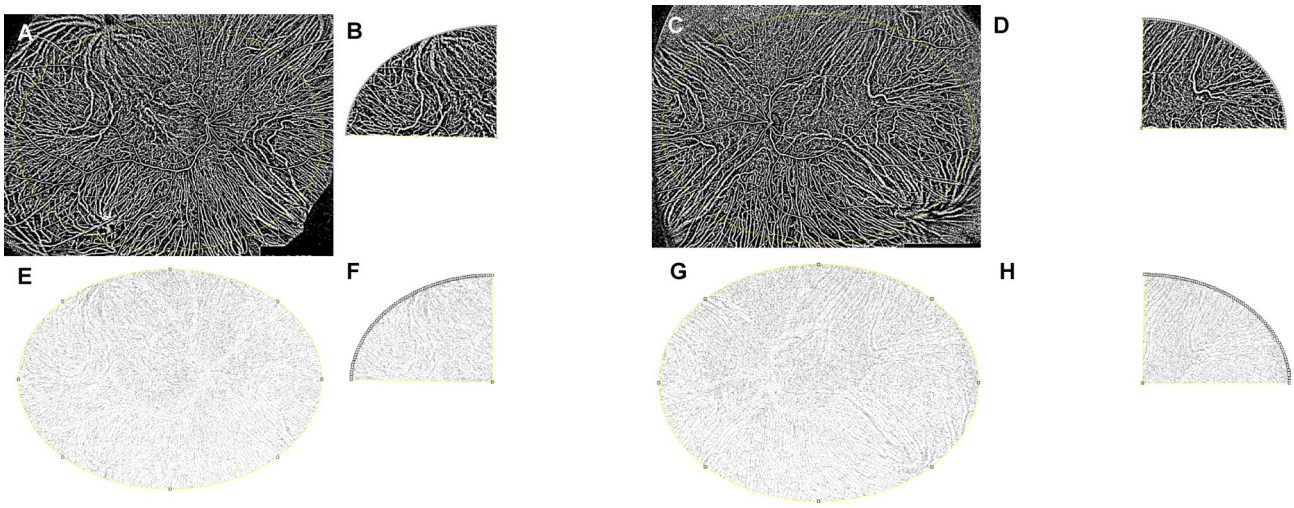

Fig. 4. Choroidal vascular density (CVD) and choroidal vascular fractal dimension (CFD) analysis using ultra-widefield indocyanine green angiography (UWF-ICGA) images of a 62-year-old female patient with superotemporal branch retinal branch vein occlusion (BRVO) in her right eye and a history of hypertension and hyperlipidemia. The top row shows CVD measurements (**A**–**D**), and the bottom row shows CFD measurements (**E**–**H**). Full quadrant analyses are presented in **A**, **C**, **E**, and **G**, while sub-quadrant analyses are presented in **B**, **D**, **F**, and **H**. Panels **B** and **F** correspond to the affected superotemporal quadrant of the right eye, and panels **D** and **H** correspond to the horizontally symmetric quadrant of the fellow eye. Whole-eye CVD values were comparable between the right (62.93; **A**) and left (62.26; **C**) eyes; however, the affected quadrant in the right eye demonstrated higher CVD (63.10; **B**) compared with its horizontally symmetric quadrant in the fellow eye (61.87; **D**). Whole-eye CFD values were also similar between the right (1.790; **E**) and left (1.798; **G**) eyes, whereas the affected quadrant in the right eye showed reduced CFD (1.785; **F**) compared with its horizontally symmetric quadrant in the fellow eye (1.824; **H**).

Data availability

The datasets generated and/or analyzed during the current study are available from the corresponding author on reasonable request.

Received: 22 August 2025; Accepted: 15 December 2025
Published online: 23 December 2025

References

1. Klein, R. The 15-Year cumulative incidence of retinal vein occlusion. *Arch. Ophthalmol.* **126**, 513. https://doi.org/10.1001/archopht.126.4.513 (2008).
2. Wong, T. Y. & Scott, I. U. J. N. E. J. o. M. Retinal-vein occlusion. **363**, 2135–2144 (2010).
3. Tsuiki, E., Suzuma, K., Ueki, R., Maekawa, Y. & Kitaoka, T. Enhanced depth imaging optical coherence tomography of the choroid in central retinal vein occlusion. *Am. J. Ophthalmol.* **156**, 543–547e541. https://doi.org/10.1016/j.ajo.2013.04.008 (2013).
4. Mitamura, Y. et al. Changes in choroidal structure following intravitreal Aflibercept therapy for retinal vein occlusion. *Br. J. Ophthalmol.* **105**, 704–710. https://doi.org/10.1136/bjophthalmol-2020-316214 (2021).
5. Rayess, N. et al. Baseline choroidal thickness as a short-term predictor of visual acuity improvement following antivascular endothelial growth factor therapy in branch retinal vein occlusion. *Br. J. Ophthalmol.* **103**, 55–59. https://doi.org/10.1136/bjophthalmol-2018-311898 (2019).
6. Okamoto, M., Yamashita, M., Sakamoto, T. & Ogata, N. Choroidal blood flow and thickness as predictors for response to Anti-Vascular endothelial growth factor therapy in macular edema secondary to branch retinal vein occlusion. *Retina* **38**, 550–558. https://doi.org/10.1097/IAE.0000000000001566 (2018).
7. Chirco, K. R., Sohn, E. H., Stone, E. M., Tucker, B. A. & Mullins, R. F. Structural and molecular changes in the aging choroid: implications for age-related macular degeneration. *Eye (Lond).* **31**, 10–25. https://doi.org/10.1038/eye.2016.216 (2017).
8. Imamura, Y., Fujiwara, T., Margolis, R. & Spaide, R. F. Enhanced depth imaging optical coherence tomography of the choroid in central serous chorioretinopathy. *Retina* **29**, 1469–1473. https://doi.org/10.1097/IAE.0b013e3181be0a83 (2009).
9. Kim, Y. T., Kang, S. W. & Bai, K. H. Choroidal thickness in both eyes of patients with unilaterally active central serous chorioretinopathy. *Eye* **25**, 1635–1640. https://doi.org/10.1038/eye.2011.258 (2011).
10. Lutty, G. A. Diabetic choroidopathy. *Vis. Res.* **139**, 161–167. https://doi.org/10.1016/j.visres.2017.04.011 (2017).
11. Choi, S. U., Kim, Y. J., Lee, J. Y., Lee, J. & Yoon, Y. H. Qualitative and quantitative evaluation of diabetic choroidopathy using ultra-widefield indocyanine green angiography. *Sci. Rep.* https://doi.org/10.1038/s41598-023-29216-5 (2023).
12. Hayreh, S. S. Retinal vein occlusion. *Indian J. Ophthalmol.* **42**, 109–132 (1994).
13. Rogers, S. L. et al. Natural history of branch retinal vein occlusion: An evidence-based systematic review. *Ophthalmology* **117**, 1094–1101. https://doi.org/10.1016/j.ophtha.2010.01.058 (2010).
14. Scott, I. U., Campochiaro, P. A., Newman, N. J. & Biousse, V. Retinal vascular occlusions. *Lancet* **396**, 1927–1940. https://doi.org/10.1016/S0140-6736(20)31559-2 (2020).
15. Ryu, G., Park, D., Lim, J., Van Hemert, J. & Sagong, M. Macular microvascular changes and their correlation with peripheral nonperfusion in branch retinal vein occlusion. *Am. J. Ophthalmol.* **225**, 57–68. https://doi.org/10.1016/j.ajo.2020.12.026 (2021).

16. Chen, L., Yuan, M., Sun, L. & Chen, Y. Choroidal thickening in retinal vein occlusion patients with serous retinal detachment. *Graefe's Archive Clin. Experimental Ophthalmol.* **259**, 883–889. https://doi.org/10.1007/s00417-020-04983-3 (2021).
17. Hwang, B. E., Kim, M. & Park, Y. H. Role of the choroidal vascularity index in branch retinal vein occlusion (BRVO) with macular edema. *PLOS ONE.* **16**, e0258728. https://doi.org/10.1371/journal.pone.0258728 (2021).
18. Aribas, Y. K., Hondur, A. M. & Tezel, T. H. Choroidal vascularity index and choriocapillary changes in retinal vein occlusions. *Graefes Arch. Clin. Exp. Ophthalmol.* **258**, 2389–2397. https://doi.org/10.1007/s00417-020-04886-3 (2020).
19. Yang, Q. et al. Flow and ischemic changes in retina and choroid across diabetic retinopathy spectrum: A SS-OCTA study. *Eye (Lond).* **39**, 1631–1640. https://doi.org/10.1038/s41433-025-03639-y (2025).
20. Guan, L. et al. Choroidal vascular alterations in diabetic retinopathy and their association with macular microvascular parameters. *Sci. Rep.* **15**, 29381. https://doi.org/10.1038/s41598-025-13414-4 (2025).
21. Ip, M. & Hendrick, A. Retinal vein occlusion review. *Asia Pac. J. Ophthalmol. (Phila).* **7**, 40–45. https://doi.org/10.22608/APO.2017442 (2018).
22. Ryu, G., Noh, D., van Hemert, J., Sadda, S. R. & Sagong, M. Relationship between distribution and severity of non-perfusion and cytokine levels and macular thickness in branch retinal vein occlusion. *Sci. Rep.* **11**, 271. https://doi.org/10.1038/s41598-020-79522-5 (2021).
23. Kim, S. A. et al. Retinal VEGFA maintains the ultrastructure and function of choriocapillaris by preserving the endothelial PLVAP. *Biochem. Biophys. Res. Commun.* **522**, 240–246. https://doi.org/10.1016/j.bbrc.2019.11.085 (2020).
24. Rayess, N. et al. Baseline choroidal thickness as a predictor for treatment outcomes in central retinal vein occlusion. *Am. J. Ophthalmol.* **171**, 47–52. https://doi.org/10.1016/j.ajo.2016.08.026 (2016).
25. Tsuiki, E., Suzuma, K., Ueki, R., Maekawa, Y. & Kitaoka, T. Enhanced depth imaging optical coherence tomography of the choroid in central retinal vein occlusion. *Am J Ophthalmol* **156**, 543–547 (2013). https://doi.org/10.1016/j.ajo.2013.04.008
26. Kim, Y. H. & Oh, J. Choroidal thickness profile in chorioretinal diseases: Beyond the macula. *Front. Med.* **8**, 797428. https://doi.org/10.3389/fmed.2021.797428 (2021).
27. Cheung, C. M. G. et al. Pachychoroid disease: Review and update. *Eye (Lond).* **39**, 819–834. https://doi.org/10.1038/s41433-024-03253-4 (2025).
28. Margolis, R. & Spaide, R. F. A pilot study of enhanced depth imaging optical coherence tomography of the choroid in normal eyes. *Am. J. Ophthalmol.* **147**, 811–815. https://doi.org/10.1016/j.ajo.2008.12.008 (2009).
29. Fan, W. et al. Relationship between retinal fractal dimension and nonperfusion in diabetic retinopathy on Ultrawide-Field fluorescein angiography. *Am. J. Ophthalmol.* **209**, 99–106. https://doi.org/10.1016/j.ajo.2019.08.015 (2020).
30. Agrawal, R. et al. Choroidal vascularity index as a measure of vascular status of the choroid: measurements in healthy eyes from a population-based study. *Sci. Rep.* **6**, 21090. https://doi.org/10.1038/srep21090 (2016).
31. Ryu, G., Moon, C., van Hemert, J. & Sagong, M. Quantitative analysis of choroidal vasculature in polypoidal choroidal vasculopathy using ultra-widefield indocyanine green angiography. *Sci. Rep.* **10**, 18272. https://doi.org/10.1038/s41598-020-75506-7 (2020).

Author contributions

Conception and design: S.U.C., Y.H.Y., and J.L.Analysis and interpretation: S.U.C., S.H., and J.L.Data collection: S.U.C., S.H., Y.J.K., and J.L.Writing–original draft: S.H. and S.U.C. Writing–review and editing: S.H., S.U.C., and J.L. Overall responsibility: S.H., S.U.C., and J.L.

Funding

This research was supported by a grant of the Korea Health Technology R&D Project through the Korea Health Industry Development Institute (KHIDI) funded by the Ministry of Health & Welfare, Republic of Korea (grant number: RS-2024-00438689), and the Asan Institute for Life Sciences, Asan Medical Center, Seoul, Korea (2023IP0079-2).

Competing interests

The authors declare no competing interests.

Additional information

Correspondence and requests for materials should be addressed to J.L.

Reprints and permissions information is available at www.nature.com/reprints.

Publisher's note Springer Nature remains neutral with regard to jurisdictional claims in published maps and institutional affiliations.